Supporting Information -

'Rheology and Dynamics of Colloidal Superballs'

Synthesis of hollow silica superballs

Milli-Q filtered water is used in all synthesis and washing steps, other reagents are used as received. Hematite superballs are prepared by first dissolving 54 g of $Fe_2Cl_3 \cdot 6H_2O$ in 100 mL of water in a 250 mL screw-top bottle, then slowly adding a solution of 21.5 g of NaOH dissolved in 90 mL of water while stirring the mixture with a magnetic stir bar. After the addition is complete, the magnetic stirring continues for 5 min then the stir bar is removed and the bottle sealed and placed in a pre-heated oven at 100 °C. The bottle is left undisturbed in the oven for 8 d, during which time hematite particles nucleate, grow, then sediment at the bottom of the container. This procedure also produces a substantial number of thin needle-like particles which aggregate into a thick tan gel. The hematite superballs are separated from the needles and other synthesis byproducts repeatedly sedimenting the larger hematite particles and re-suspending them in water.

Before coating the hematite superballs with silica, we first non-specifically absorb polyvinylpyrrolidone (PVP-10) to the hematite surface by mixing the hematite superballs with a concentrated solution of 20 g PVP-10 dissolved in 200 mL water. To prevent aggregation and ensure a uniform PVP coating, the superball - PVP mixture is sonicated for 3 hours, and then magnetically stirred overnight. The hematite particles are again repeatedly sedimented and re-suspened in water to remove excess PVP, then finally suspended in ethanol. Prior to coating, we image small samples of the hematite superballs with TEM and optical microscopy to verify the colloidal stability and check that there are no remaining needles stuck to the superballs. If we find a significant number of needles stuck to the hematite or if the superballs stick together in irreversible aggregates, we repeat the PVP coating and washing process until we obtain clean, stable hematite particles.

For fluorescent silica shells, a dye solution is prepared ahead of time by dissolving 0.079 g Rhodamine B isothyocynate (RITC) in 2 mL (3-Aminopropyl)trimethoxysilane (APS) and 10 mL ethanol. This solution is mixed with a magnetic stirrer for at least 24 h then stored in a refrigerator until need. The silica coating is performed in a 3 L three neck flask held fixed in a large, temperature controlled sonication bath with an overhead mixer suspended above. First, 1.5 L of ethanol is mixed in the flask with 10 mL water and 66 mL of a 1 % by volume solution of tetramethyl ammoniumhydroxide (TMAH) in water. While sonicating and stirring from above, 100 g of the hematite particle suspension (in ethanol at a concentration of 0.5 % by mass) is then added to the flask. Additional ethanol (40 mL to 50 mL) is added to flush any hematite particles that may have stuck to the walls of the flask. Continuing the stirring and sonication, a mixture of 5 mL tetraethylorthosilicate (TEOS), 4 mL of the dye solution

and 1 mL ethanol is slowly dripped in using a syringe pump at a rate of 1.8 mL/h. After this addition step, a small sample of hematite particles is collected, washed, and checked with fluorescence microscopy to make sure the dyed silica is absorbing to the particles. After this, we add a solution of 5 mL TEOS and 5 mL ethanol at the same 1.8 mL/h flow rate. For undyed cubes, the dye solution is omitted and simply two additions of 5 mL TEOS and 5 mL ethanol are performed. About 30 minutes after the TEOS addition is complete, a solution of 20 g PVP is dissolved in 200 mL ethanol and added to the flask. The combination of stirring and sonicating continues for two more hours, then the sonicator is turned off and the stirring continues overnight.

The following day, the coated particles are washed three to four times with ethanol then four more times with water. The coated cubes are then be transferred to a concentrated 18.5 % solution of HCl and stirred to dissolve the hematite cores. As the concentration of dissolved iron increases, the etch rate of the hematite slows down, so the acid solution is replaced via sedimentation and resuspension every two to three hours to speed the etching process. It typically takes 24 h to complete the etching process, after which the silica shells are washed multiple times with water until the pH is brought back up to 5 or higher. The hollow, silica superballs are then transferred to ethanol for long term storage until needed.

Index matching and sample preparation

We prepare index-matched suspensions of silica superballs in a glycerol/water suspending fluid for use in both confocal and rheological measurements. The superballs are first washed 10 times with water adjusted to a pH of 9 with a small amount of TMAH to slightly charge the silica and suppress aggregation. They are then transferred to the glycerol/water mixture, repeatedly sedimenting the superballs via centrifugation and replacing the supernatant to tune the refractive index. The index of refraction of spherical silica colloids can vary depending on the synthesis details but usually falls somewhere between 1.42 and 1.47, requiring a high glycerol concentration for index matching.

The hollow nature of the silica superballs presents a challenge for precise index matching, since one must allow the outer fluid adequate time to permeate the silica shells. The flow rate through the porous shell depends on the fluid viscosity and osmotic pressure difference, and hence slows significantly as the glycerol content increases. We limit ourselves to only one or two supernatant swaps per day, slowly increasing the glycerol content and judging the quality of the index matching based on visual inspection of concentrated superball suspensions. Slowly carrying out this procedure over roughly two weeks, we found that the superballs were well matched in a mixture with $n = 1.461$, corresponding to a 92 % by mass glycerol/water mixture.

To obtain a rough estimate for the timescale for diffusion though the silica shells, we prepared an index-matched suspension of undyed superballs and then, after a week in the glycerol/water mixture, added a small amount of fluorescene sodium salt to fluorescently dye the outer fluid. In confocal images we observe little diffusion of dyed outer fluid into the undyed superballs over the course of a week, though after about two months enough dye had diffused in to the superballs to render them nearly invisible. This indicates that the timescale for the outer fluid to diffuse through the silica shell is far slower than the timescale for colloidal

diffusion, so that the superballs can be regarded as impermeable over the course of the diffusion and viscosity measurements.

Sedimentation

Density matching silica is difficult,[1] and in this work we have prioritized index matching to facilitate 3D confocal imaging and minimize attractive interactions. We can characterize the relative importance of sedimentation and Brownian motion using the gravitational Péclet number $Pe_g \equiv \Delta mga/k_BT$, which is the ratio of potential energy needed to raise a particle its own diameter Δmga compared to the thermal energy k_BT. Here $\Delta m = \Delta\rho v_p$, with v_p the solid particle volume and $\Delta\rho \approx 1$ g/cm^3 the density difference between the solid and suspending fluid. For the solid silica spheres $Pe_g \approx 3.3$, indicating that diffusion and sedimentation were roughly comparable in magnitude. Comparing the relevant timescales for shear-induced diffusion[2] $\tau_{shear} \propto 1/\dot{\gamma}$ and sedimentation $\tau_{sed} \propto u_{sed}/a \propto \Delta\rho ga/\mu$ we find that $\tau_{shear}/\tau_{sed} \propto \Delta\rho a/\mu\dot{\gamma} \approx 10^{-1}$ to 10^{-4} for the range of shear rates explored here ($\mu = 0.025$ Pa·s for the 70 % mass fraction glycerol/water mixture). This indicates that sedimentation has a minimal influence on the observed rheology, which is supported by the lack of observed time-dependence in the measured viscosity or hysteresis when increasing and decreasing the shear rate.

Sedimentation slower in the hollow silica superballs, since Δm only depends on the volume of the physical shell. We estimate the shell thickness to be about 60 nm giving us $Pe_g \approx 0.7$, a factor of four smaller than in the solid silica spheres (assuming the same $\Delta\rho$). The viscosity of the superball index matching fluid is roughly a factor of 10 larger than the viscosity of the silica sphere index matching fluid so τ_{shear}/τ_{sed} is a factor of 40 smaller in the superball suspensions, making sedimentation even less of a concern in the superball rheology.

The PMMA spheres were not perfectly density matched and also slowly sedimented under gravity. While we do not precisely know $\Delta\rho$, we measured the sedimentation velocity in dilute suspensions to be $u_{sed} \approx 0.02$ μm/s. From this we estimate $Pe_g = u_{sed}a/D_0 \approx 0.2$, smaller than in the superball suspensions.

After removing the average drift in each direction (common practice when computing MSDs), we did not observe any consistent anisotropy in the particle mean squared displacements in the individual x, y or z directions, indicating that the particle diffusion was isotropic and not strongly influenced by the slow sedimentation. We were unable to obtain fluorescent solid silica spheres that were sufficiently bright for direct tracking. Precisely tracking undyed spheres against a dyed background fluid proved challenging, particularly in dilute suspensions. For this reason, we only used PMMA spheres for the hard-sphere diffusion measurements.

Separating hydrodynamic and structural contributions to the viscosity

As noted in the main text, while we can rescale the packing density to $\phi \rightarrow \phi_{eff}$ to bring the hard sphere and superball diffusion measurements into rough agreement, applying this rescaling to the viscosity is not straightforward. This is because the corrections

to the diffusion at finite packing density depend directly on the particle interactions and suspension microstructure (through $g(r)$) but the ϕ dependent contributions to the viscosity contain independent contributions from the single particle hydrodynamics as well as the microstructure.

This can be seen most clearly in the theoretical and numerical work by refs.[3,4] which address the rheology of 'effective hard sphere' particles with a hydrodynamic radius a and a larger hard sphere radius $b > a$, with b playing the role of a_{eff} in our work. By consider only two-body interactions, it is possible to numerically solve the two-particle Smoluchowski equation for the non-equilibrium pair distribution $g(r)$ at arbitrary Péclet number Pe. This pair distribution is then used to evaluate the two-particle contributions to the hydrodynamic and Brownian contributions to the stress, so the results derived in this work only include viscosity corrections up to $O(\phi^2)$ but should valid for all shear rates. The hydrodynamic contributions to the shear stress (which are the dominant contributions at high shear rates) take the form (see Eq. 3.6 from[3])

$$\Sigma^H_{shear} = \frac{5}{2}\phi\mu\dot{\gamma} + \frac{5}{2}\phi^2\mu\dot{\gamma} + \phi\phi_b\mu\dot{\gamma}\int d\vec{r}' g(\vec{r}')H_{shear}(\vec{r}') \tag{1}$$

where $\vec{r}' = \vec{r}/b$ so the integral in the last term is dimensionless and $H_{shear}(\vec{r}')$ contains numerous hydrodynamic functions that describe the two-particle hydrodynamics. The packing density $\phi = \frac{4}{3}\pi a^3 n$ is set by the hydrodynamic radius a while $\phi_b = \frac{4}{3}\pi b^3 n = (b/a)^3\phi$ is set by the larger effective hard-sphere radius (analogous to ϕ_{eff}). The linear term in Eq. (1) is proportional to ϕ and the coefficient is the hard-sphere intrinsic viscosity $[\eta]^{HS} = 5/2$. This term is completely independent of b, reflecting the fact that $[\eta]$ is determined by the hydrodynamic stresses around a single particle[5,6] and independent of the suspensions microstructure. The next term contributes $[\eta]\phi^2$ to the relative viscosity, indicating a purely hydrodynamic contribution to the ϕ^2 correction as well. The final term in Eq. (1) is proportional to $\phi\phi_b$, representing a mixed term that combines hydrodynamics and structure.

This suggests that the relative viscosity in the high-shear regime should take the form

$$\eta_N/\mu = 1 + [\eta]\phi + [\eta]\phi^2 + c_{a,b}\phi\phi_b + ... \tag{2}$$

where $c_{a,b}$ is set by the mixed term in the hydrodynamic stress. This is very similar to results for charged spheres, where the relative viscosity contains $[\eta]\phi$ and $[\eta]\phi^2$ contributions plus a ϕ^2 contribution that depends on strength of the electrostatic interactions.[5] It is not obvious how the higher order terms should scale, but based on the two-particle contributions we might expect the three-particle interaction to contribute terms of the form $c_{a,a,b}\phi^2\phi_b$ as well as $c_{a,b,b}\phi\phi_b^2$.

These mixed terms prevent any simple rescaling of the superball viscosity analogous to the rescaling of $D_L(\phi) \rightarrow D_L(\phi_{eff})$.

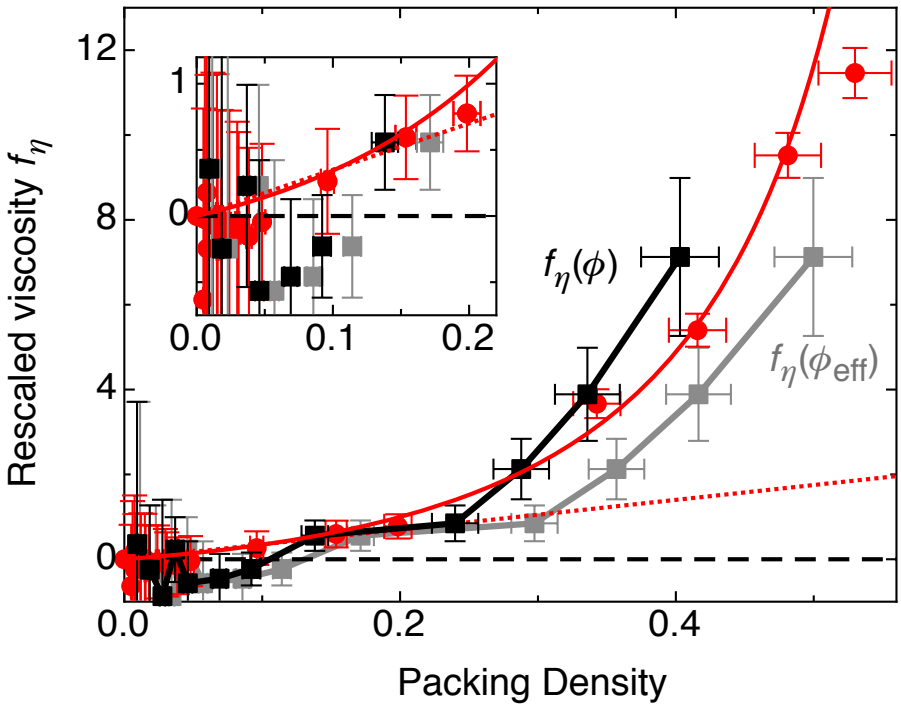

Fig. 1 Rescaled viscosity f_η (defined by Eq. 3) for spheres (red circles) and superballs (squares). Black squares: f_η plotted against the physical packing density ϕ. Gray squares: plotted against the effective packing density ϕ_{eff}. Also shown is f_η for hard spheres using $\eta_N/\mu = (1-\phi/\phi_m)^{-[\eta]\phi_m}$ with $[\eta] = 2.5$ and $\phi_m = 0.71$ (solid red line) and to $O(\phi^2)$ $\eta_N/\mu = 1+2.5\phi+6.0\phi^2$ (dotted red line). Error bars in reflect variations in η over the course of repeated up and down shear sweeps as well as uncertainty in the viscosity of the suspending fluid.

We can remove the known hydrodynamic contributions from the viscosity

$$f_\eta = \frac{\eta_N/\mu - (1+[\eta]\phi+[\eta]\phi^2)}{\phi} = c_{a,b}\phi_b + \ldots \tag{3}$$

but mixed terms still persist at higher orders. Since we know $[\eta]$ for the superballs, in principle we can compute f_η to attempt to isolate the structural contributions to the $O(\phi^2)$ term in the viscosity. However in practice this is challenging, since this contribution will be vanishingly small at low ϕ while mixed higher order terms will prevent any simple scaling at higher packing densities.

We attempt this rescaling in Fig. 1, plotting $f_\eta(\phi)$ and $f_\eta(\phi_{eff})$ for the superballs (using $[\eta] = 2.55$) and f_η for our silica spheres (using $[\eta] = 2.5$). To gauge the relative contributions of second order and higher order terms, we also plot f_η using analytic expressions for η_N/μ established in hard sphere suspensions. Using a Kreiger-Dougherty type equation (Eq. 3 from the main text) for η_N/μ with $[\eta] = 2.5$ and $\phi_m = 0.71$, we capture the viscosity in both the dilute and high packing density limit (solid red line). To highlight the $O(\phi^2)$ contributions, we plot f_η using 2nd order expansion of the hard sphere high-shear viscosity $\eta_N/\mu = 1+2.5\phi+6.0\phi^2$, giving $f_\eta = 3.5\phi$ (dotted red line). Comparing these two expressions, we see that higher order

contributions become significant when $\phi > 0.2$.

Below $\phi \approx 0.1$ our uncertainty in both the sphere and superball data is too large to draw any conclusions. For $0.1 < \phi < 0.2$ we can begin to resolve the ϕ^2 contributions, though both $f_\eta(\phi)$ and $f_\eta(\phi_{eff})$ are consistent with the hard sphere results. At higher packing densities neither $f_\eta(\phi)$ nor $f_\eta(\phi_{eff})$ for the superballs matches the hard sphere f_η, with $f_\eta(\phi)$ rising above the sphere results and $f_\eta(\phi_{eff})$ falling below.

References

1 C. P. Royall, W. C. K. Poon and E. R. Weeks, *Soft Matter*, 2013, **9**, 17–27.

2 R. J. Phillips, R. C. Armstrong, R. A. Brown, A. L. Graham and J. R. Abbott, *Phys. Fluids A*, 1992, **4**, 30–40.

3 J. Bergenholtz, J. F. Brady and M. Vicic, *J. Fluid Mech.*, 2002, **456**, 239–275.

4 B. Cichocki, M. L. Ekiel-Jeżewska and E. Wajnryb, *Colloid Surface A*, 2013, **418**, 22–28.

5 W. Russel, D. Saville and W. Schowalter, *Colloidal Dispersions*, Cambridge University Press, 1992.

6 J. Mewis and N. Wagner, *Colloidal Suspension Rheology*, Cambridge University Press, 2011.